This paper was published in Microsystem Technologies 20 (4-5), 2014, pp. 919-925
The original publication is available at www.springerlink.com

# Evaluation of bioinspired functional surfaces for nanoparticle filtering

Sebastian Busch[a]*, Manuel Ketterer[a], Xenia Vinzenz[b], Christian Hoffmann[b], Katrin Schmitt[c], Jürgen Wöllenstein[a,c]

[a]Department of Microsystems Engineering IMTEK, University of Freiburg, Freiburg, Germany; [b]Institute for Bioprocessing and Analytical Measurement Techniques, Heilbad Heiligenstadt, Germany; [c]Fraunhofer Institute for Physical Measurement Techniques, Freiburg, Germany

## ABSTRACT

We present the development of a novel integrated device for airborne nanoparticle filtering with bioinspired nanoscale functionality. The underlying idea is to investigate the principle of adherent surfaces, e.g. pollen, as a biological model and transfer this functionality into a technology using functionalized microstructured surfaces. This might offer an efficient filtering method for nanoscale airborne particles without the limitations in gas permeability of conventional filters. We investigated the different pollen species for their structural and biochemical surface properties to achieve bioinspired surface functionality on silicon surfaces. The resulting conical structures have sizes from 4-20µm. Depending on structure sizes, the adhesive properties of the surfaces towards aerosol particles could be directly influenced. The surfaces were tested in a demonstrator setup and the collection efficiency visually determined.

**Keywords:** pollen surface, particle filter, fine dust

## 1. INTRODUCTION

Today we feel for many reasons that the pollution of our environment with unconsciously released nanoparticles is steadily increasing. In recent years, a number of studies have revealed more and more adverse health effects of both naturally occurring and anthropogenic airborne nanoparticles – a commonly known example is the fine dust in the exhaust gas of vehicles. Exhaust gas from diesel engines contains a large quantity of possibly harmful nanoparticles, caused by incomplete combustion of fuel. Yet also current filtering techniques come to their limitations concerning the elimination of fine particles in the nanometer size range, or even produce toxic byproducts such as benzene, toluene, dioxin and furan during the regeneration cycle (Heeb et al. 2005). Many studies have already reported a connection between the increasing prevalence of respirable dust in the environment and the frequency and the degree of hypersensitivity reactions in humans. Type I hypersensitivity reactions, such as rhinitis allergies and allergic asthma, are the most common allergic diseases. At the same time, an increasing number of people suffers from allergies, e.g. against pollen. First hints have now been given that agglomerates of fine dust sticking on pollen surfaces render them more aggressive against the human immune system (Gruijthuijsen et al. 2006; Behrendt and Becker 2001; Chehregani and Kouhkan 2008; Chehregani et al. 2004).

Pollen grains are the male gametes of higher plants, having sizes between a few and a few hundred µm. One focus of research is the chemical composition of the pollenkitt (Hesse 1981; Hesse 1980/1; Hesse 1980/2; Pacini and Hesse 2005), which is responsible for the adhesion of pollen to pollinators, or the agglomeration of pollen themselves. In general, the pollen coat consists of a cellulose rich wall, the intine integrating also some enzymes and other proteins, and the chemically very stable outer wall, composed largely of sporopollenin of which the chemical composition is still not exactly known (Heizmann et al. 2000; Luu et al. 1997; Luu et al. 1999; Murphy 2006; Zinkl et al. 1999). Among its components is a mixture of biopolymers containing mainly long chain fatty acids, phenylpropanoide (plant-derived organic compounds biosynthesized from the amino acid phenylanaline) and phenolics. If fine dust adheres to the pollen surface, the pollen starts germinating, altering its surface composition. In this state, allergic reactions in humans are activated significantly faster. With scanning electron microscopy, the increasing threat of the recent years can be revealed. An example is shown in Fig. 1, with native pollen (Fig. 1a) compared to pollen exposed to a fine dust sample (Fig. 1b).

*sebastian.busch@imtek.uni-freiburg.de; phone +49 761 203-67583; fax +49 761 203-67684; www.imtek.de

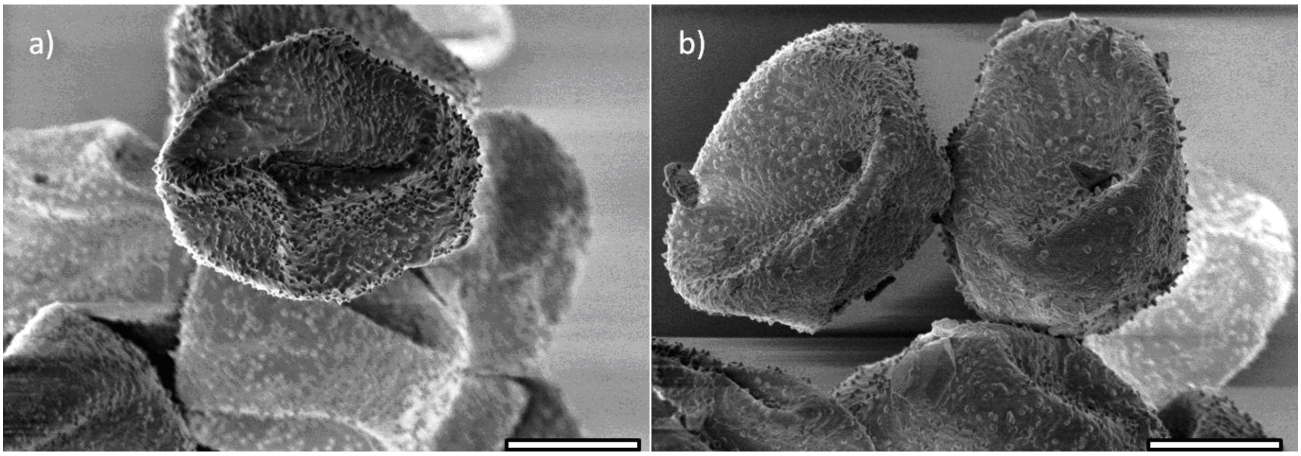


Figure 1: SEM images of paper mulberry pollen (*Broussonetia papyrifera*) b) mulberry pollen mixed with road dust adhering to the pollen surface (Scale bar = 5µm)

These observations lead us to the idea of a translation of the surface properties of different pollen to intentionally capture airborne nanoparticles on functional technical surfaces. The underlying hypothesis is that such bioinspired technical surfaces, i.e. resembling the biological model, possibly work as efficient capturing method for airborne nanoparticles. The aim of our study was to develop a simple process of fabricating functional microstructured surfaces mimicking the adhesive properties of pollen surfaces and show a proof-of-principle that these surfaces are able to capture small particles from an airflow.. These surfaces could serve as a basis for filter elements for pollutant fine dust. Conventional filters impose a challenge in filtering airborne particles with sizes below 1µm, where they need to achieve a high efficiency while maintaining gas permeability. We intend to combine the results of exine morphology and dominating functional groups on the pollen surface to translate both structural and biochemical information into a technical surface based on silicon microtechnology carrying a functional coating. Such coatings can, for example, be achieved with layer-by-layer (LbL) deposition of polyelectrolytes due to their applicability to substrates of different shapes and sizes, while the self-assembling layers are formed under mild conditions (Vinzenz 2012). In a first step, we present the evaluation of suitable biological models, i.e. pollen, the transfer of similar structures to Si-based surfaces, and the evaluation of the adhesive properties of bioinspired structured surfaces towards fine dust in a demonstrator setup. The advantage of these structured surfaces is that a filter element can be set up as surface filter, which allows higher gas permeability than flow-through filters. Next steps will include the application of different functional coatings.

# 2. EXPERIMENTAL

## 2.1 Scanning electron microscopy

Pollen samples of daisy (*Bellis perennis*) and pine (*Pinus sylvestris*) were collected in southern Germany during flowering season and spread on carbon black tape for scanning electron microscopy in their native, dehydrated state without further preparation. Paper mulberry (*Broussonetia papyrifera*) pollen sized 11.2-16.4µm was obtained from Duke Scientific (Palo Alto, USA) and prepared identically. Scanning electron microscopy (Hitachi SU 70) was performed using an acceleration voltage of 1kV in case of the biological samples, 12kV on the Si surfaces.

## 2.2 Atomic force microscopy

Atomic force measurements were performed using an XE100 (Park Systems) in non-contact mode (NC-AFM). The pollen samples were spread on double-sided adhesive tape in their native state. The resolution was set to 1024 x 1024 pixels, the scanning frequency was 285kHz. The scan size, i.e. region of interest, was 2 µmx2 µm.

### 2.3 Silicon microtechnology

4-inch *p*-type, <100>-oriented silicon wafers (Si-Mat, Germany) with 525 µm ± 20 µm thickness with a resistivity of 10.0–12.2 mΩcm and 1µm $SiO_2$ passivation layer was used as substrate. All wafers were cleaned using acetone and isopropanol, rinsed with deionized water (ultrapure, ρ≥18.2 MΩ cm at 20 °C) and dried under nitrogen. A photoresist pattern of 1cm squares with circles of different radii and distances (cf. Table 1) was fabricated using optical lithography, and transferred onto the $SiO_2$ layer during 17min etching in buffered HF solution. The wafers were diced between the active areas separating the 1cm squares. All square pieces were further etched in solutions containing different concentrations of potassium hydroxide and isopropanol. Table 1 gives the composition of the solutions and achieved radii and distances. After cleaning with acetone, the substrates were treated using plasma with 80% $N_2$/20% $O_2$ for 60 s at 40 kHz and 100 W (Diener Plasma, Germany) to remove all organic residues. Subsequently, certified road dust (BCR723, Sigma-Aldrich) was applied to the surfaces in excess (approx. 1mg) and removed using pressurized $N_2$. The samples were again examined using SEM and adherent particles were counted using ImageJ.

Table 1: Composition of anisotropic wet etch solutions and etch results

| *Solution #* | *40% Potassium hydroxide at 40°C* | *40% Potassium hydroxide+10% Isopropanol at 70°C* | *Radius /µm* | *Distance / µm* | *Description* |
|---|---|---|---|---|---|
| 1 | | 52 min | 20 | 50 | large cone |
| 2 | | 8 min | 4 | 10 | small needle |
| 3 | 15.3min | | 4 | 10 | small cone |

### 2.4 Demonstrator setup

A demonstrator was set up for the investigation of filtering efficiency of the structured surfaces. A polypropylene box sized 30 x 80 x 15 mm³ was equipped with two lateral sliders holding at least four of the 1cm squares (structured and blank Si for reference) at 45°, two on each side. Fig. 2 shows a photograph and a schematic of the demonstrator with gas in- and outlet. A membrane filter (MN85/70, Macherey-Nagel, Germany) was placed at the gas outlet side for residual particle sampling. A total of 2mg was placed in the gas inlet directly in front of chamber as depicted in the schematic (Fig. 2b). The measurement was done three times using a new membrane filter in each run.

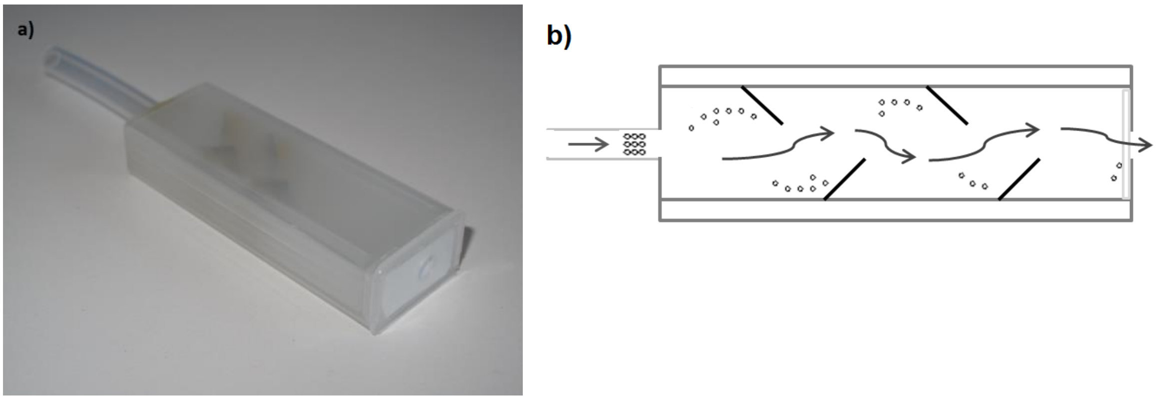


Figure 2: a) Photograph of the demonstrator system. On the left side is the gas inlet into the system, on the right outlet side the membrane filter is situated for the collection of residual particles. The schematic (b) depicts a top view of the system with the gas flow.

## 3. RESULTS AND DISCUSSION

### 3.1 Scanning electron and atomic force microscopy

Scanning electron microscopy was used to determine pollen surface morphology on the micrometer scale. Atomic force microscopy allowed the resolution of morphological details down to the nanometer scale, and the acquisition of a depth profile, i.e. the roughness. Since the pollen were used in their natural state with a high degree of dehydration, the pollen grains themselves were deformed arbitrarily; yet this did not interfere with the evaluation of microstructural features.

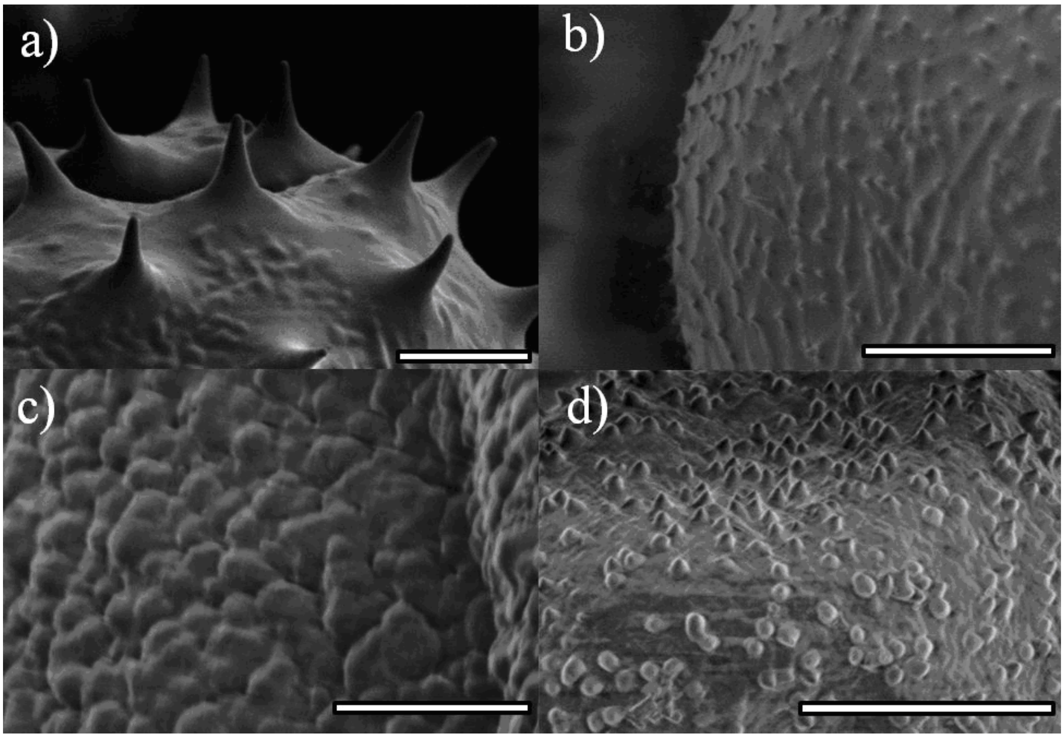


Figure 3: SEM images of pollen surfaces a) daisy (*Bellis perennis*) b) birch (*Betula sp.*) c) pine (*P. sylvestris*) d) paper mulberry (*Broussonetia papyrifera*) (scale bar =3µm)

Fig. 3 gives the SEM pictures of the three pollen species. *B. perennis* shows pronounced spines having heights of (2.5±0.1) µm (n=6) and distances from each other of (4.6±1.0) µm (n=8). The ratio of diameters at the tip/bottom is approximately 0.7. The spines are distributed evenly across the surface. The anemogamic *B. papyrifera* shows small spinules with (0.29±0.09) µm (n=7) distance from each other and (0.20±0.03) µm (n=8) height, yet spread unevenly across the surface. The anemogamic *P. sylvestris* does not have distinct spines or spinules, rather convoluted structures with sizes in the range of 1-2 µm. Further morphological detail of the anemogamic species could be achieved using AFM. Fig. 3 depicts the results of 2 µm x 2 µm AFM scans. The spinules of *B. papyrifera* (Fig. 4a) are distinct with a comparably smooth surface microstructure, whereas *P. sylvestris* (Fig. 4b) shows ultrastructural convolutions on the sub-micrometer scale. For a quantitative assessment, the average roughness Ra was evaluated across the scanned surface and determined to approx. 69.5 nm for *P. sylvestris* and approx. 0.1 nm for *B. papyrifera*.

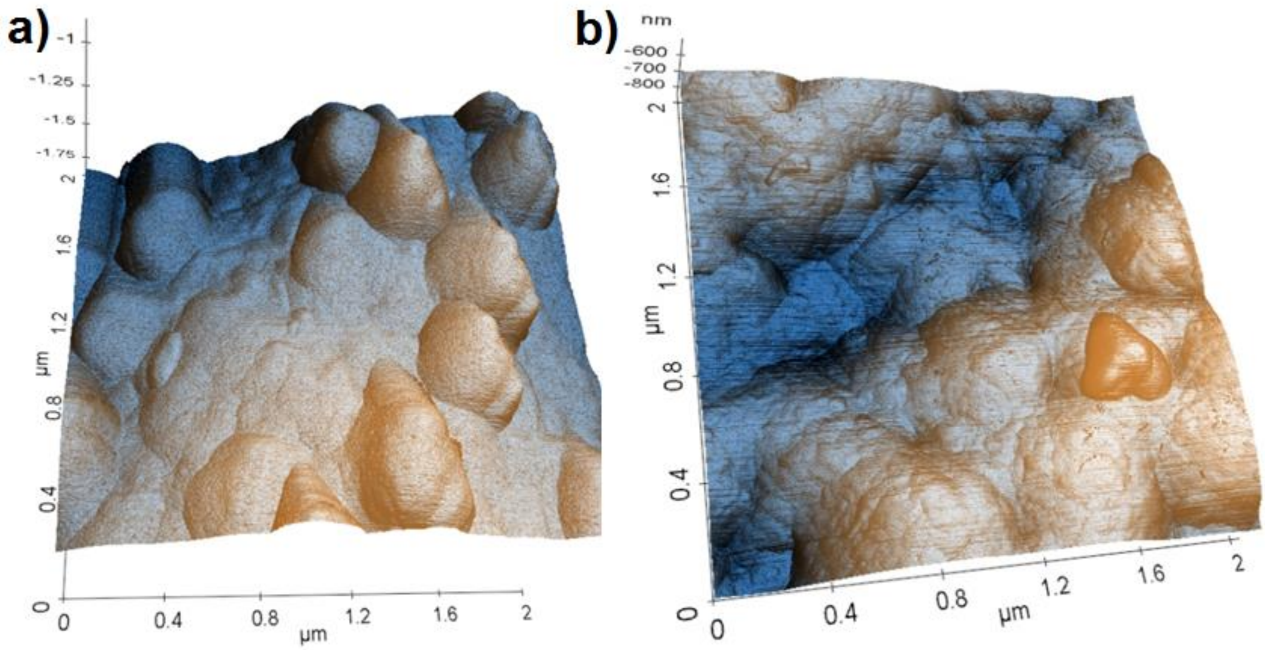


Figure 4: AFM scan (2µm x 2µm) of a) Paper Mulberry (*B. papyrifera*) pollen and b) Pine (*P. sylvestris*) pollen surface. Pine shows ultrastructural convolutions on the sub-micrometer scale

### 3.2 Silicon microtechnology

Structures etched in Si were chosen according to their pollen models, in addition one blank Si wafer was used as reference (Fig. 5a). The structure in Fig. 5b (small needles, cf. Table 1), was chosen as model for *B. perennis*, Fig. 5c shows small cones for *B. papyrifera*, and Fig. 5d shows large conical structures resembling *P. sylvestris*. The structures fabricated in Si technology resemble the structures found on the pollen surfaces, yet have slightly different dimensions which is due to the etching process used. Current work investigates the use of different etching processes (e.g. White Etch instead of KOH) to achieve smaller structural dimensions. As a result it can be noticed that the number of particles on the fabricated structured surfaces are larger than on the blank surface, yet a significantly higher number of particles adhere on the structure with the large cones compared to the others.

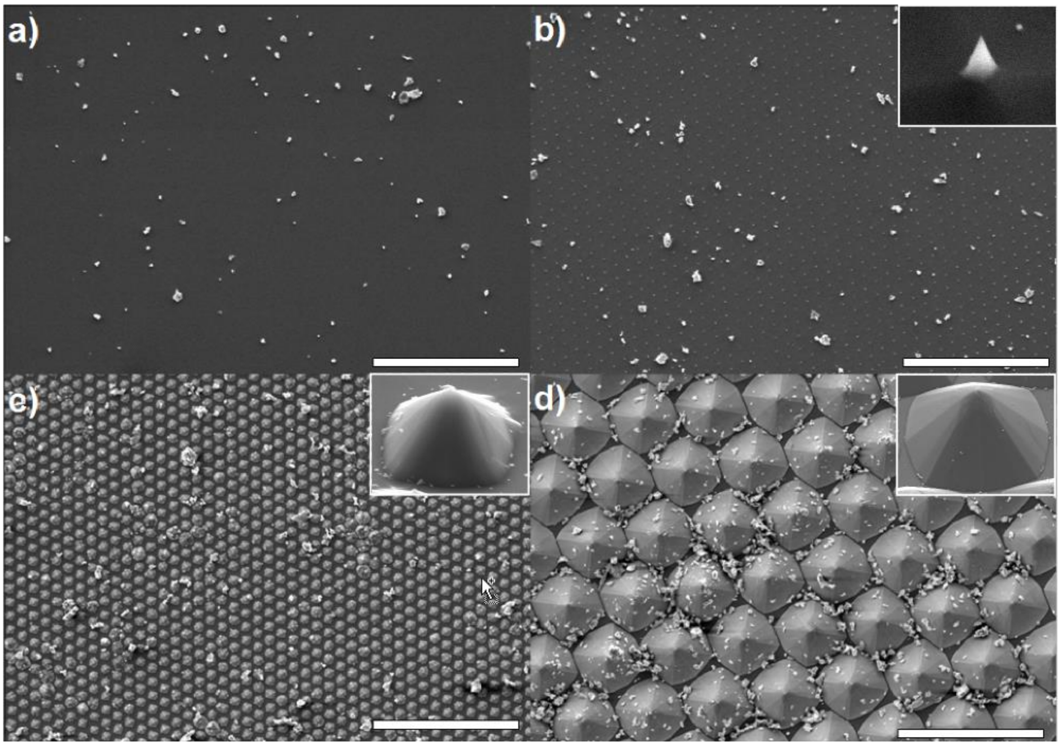


Figure 5: Etched Si surfaces with fine dust particles (scale bar = 100µm) a) blank wafer b) small needle c) small cone d) large cone structure

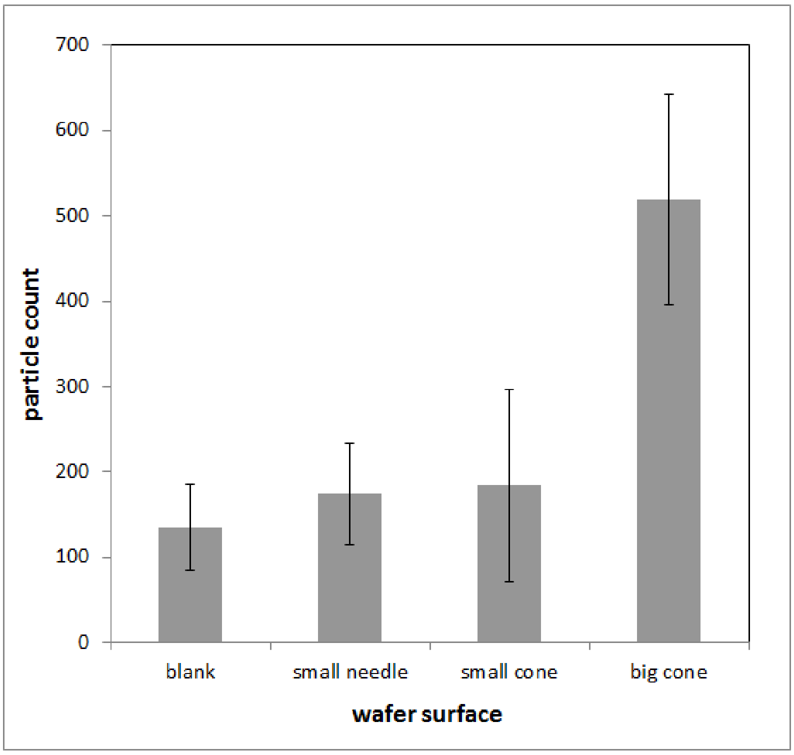


Figure 6: Comparison of the number of adherent dust particles on the structured surfaces a) blank wafer b) small needles c) small cones d) large conical structure. More than twice the amount of dust particles adheres on the large conical structure in comparison to the small needles and small cones.

### 3.3 Evaluation of structured surfaces

Fig. 7 depicts the membrane filters of the measurements using blank four Si surfaces and four structures with large cones (cf. Fig. 5). Since the membrane filters are located at the gas outlet side of the demonstrator setup, the particle load on the filters is an indirect measurement of the collection efficiency of the Si surfaces, i.e. the lower the load on the membrane filters, the higher the collection efficiency of the system. Qualitatively it can be seen that the collection efficiency is higher for the structured surface, and in both measurements the collection efficiency decreases with the number of runs. This is probably due to the fact that a comparably high load of particles was used to flow through the system and that the surfaces saturated quickly. This measurement shows the proof-of-principle that the structured surfaces are able to bind more particles in a flow-through setup, using the surfaces as surface filters, than unstructured surfaces, and we expect to increase the collection efficiency further by applying functional coatings on these surfaces. Further detailed insight into the collection efficiency of the different surfaces can be achieved by direct evaluation, e.g. measurement of mass load. Since the additional mass load of captured nanoparticles is very low compared to the filter element, a direct gravimetrical evaluation will possibly be difficult. One option can be to implement the filter elements in a resonator setup, as proposed in (Hajjam 2011; Wasisto 2012). Here structured surfaces were used to detect very small changes in mass load.

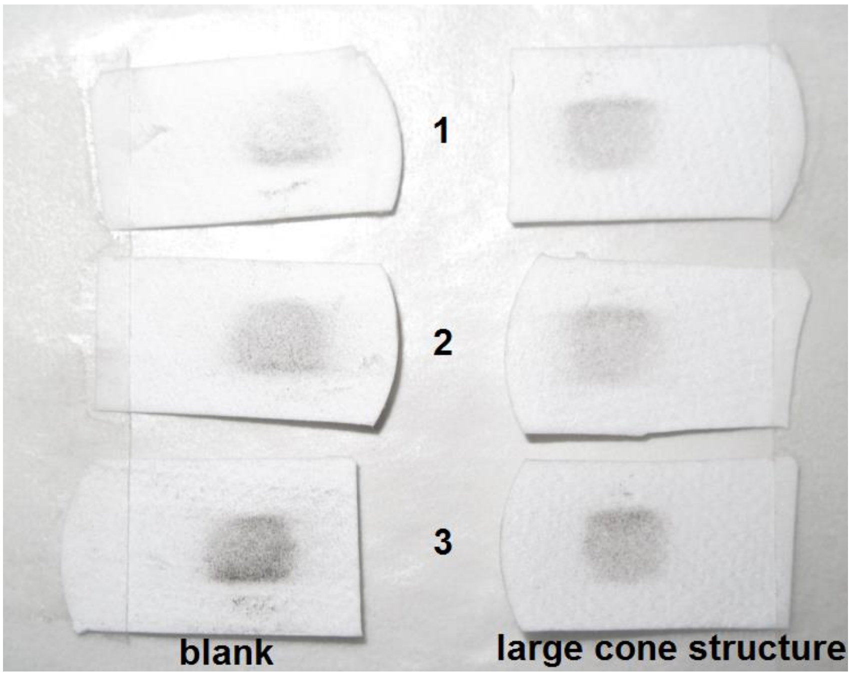


Fig. 7: Comparison of blank Si and structured surfaces upon particle flow in the demonstrator system. The membrane filters were placed at the gas outlet side of the demonstrator and indicate the collection efficiency in the system.

## 4. CONCLUSIONS AND OUTLOOK

We showed the characterization of the exine morphology of pollen surfaces for the bioinspired realization of tailor-made functional surfaces for the intentional binding of fine particles. Four structurally different pollen species were chosen as model and a simple process for the fabrication of functional microstructured surfaces was developed. We could show the proof-of-principle that the adhesive properties of the surfaces towards aerosol particles could be directly influenced depending on the surface structure. Future work will be devoted to the characterization of different functional coatings combined with adapted microstructures, fabricated with etching methods allowing further miniaturization, with regard to their ability to bind pollutant fine dust and a quantification of the collection efficiency in different setups.

## ACKNOWLEDGEMENTS

We gratefully acknowledge financial support from the German Research Foundation under grant number WO 1698/1-1. We thank Marie-Luise Bauersfeld and Carolin Peter, Fraunhofer IPM, for their assistance with photolithography and dry etching.

## REFERENCES

Behrendt H., and Becker W. M., "Localization, release and bioavailability of pollen allergens: the influence of environmental factors" Curr Opin Immunol,, 13-6, 709-715 (2001).

Chehregani, A. and Kouhkan, F. "Diesel exhaust particles and allergenicity of pollen grains of Lilium martagon.," Ecotoxicol Environ Saf, 69(3), 568-573 (2008).

Chehregani, A., Majde, A., Moin, M., Gholami, M., Ali Shariatzadeh, M. and Nassiri, H. "Increasing allergy potency of Zinnia pollen grains in polluted areas.," Ecotoxicol Environ Saf, 58(2), 267-272 (2004).

Gruijthuijsen Y.K. et al. “Nitration Enhances the Allergenic Potential of Proteins.” Int Arch Allergy Immunol, 141, 265–275 (2006).

Hajjam, A., Wilson, J.C., Pourkamali, S., “Individual air-borne particle mass measurement using high-frequency micromechanical resonators,” IEEE Sensors Journal 11 (11) 2883–2890 (2011), http://dx.doi.org/10.1109/JSEN.2011.2147301. Heeb N.V. et al. “Secondary emissions risk assessment of diesel particulate traps for heavy duty applications.“ SAE Technical Paper Series, 26, 014 (2005).

Hesse, M. "The fine structure of the exine in relation to tile stickiness of angiosperm pollen," Review of Palaeobotany and Palynology, 35, 81-92 (1981).

Hesse, M. "Ultrastruktur und Entwicklungsgeschichte des Pollenkitts von Euphorbia cyparissias, E. palustris und Mercurialis perennis (Euphorbiaceae)," Plant Systematics and Evolution, 135, 253-263 (1980).

Hesse, M. "Entwicklungsgeschichte und Ultrastruktur von Pollenkitt und Exine bei nahe verwandten entomophilen und anemophilen Angiospermensippen der Alismataceae, Liliaceae, Juncaceae, Cyperaceae, Poaceae und Araceae," Plant Systematics and Evolution, 134, 229-267 (1980).

Heizmann, P., Luu, D. T. and Dumas, C. "Pollen-Stigma Adhesion in the Brassicaceae," Annals of Botany, 85, 23-27 (2000).

Luu, D.-T., Heizmann, P. and Dumas, C. "Pollen-Stigma Adhesion in Kale 1s Not Dependent on the Self-(in) Compatibility Genotype," Plant Physiol. 115, 1221-1230 (1997).

Luu, D.-T., Marty-Mazars, D., Trick, M., Dumas, C. and Heizmanna, P. "Pollen–Stigma Adhesion in Brassica spp Involves SLG and SLR1 Glycoproteins," The Plant Cell, 11, 251-262 (1999).

Murphy, D. J. "The extracellular pollen coat in members of the Brassicaceae: composition, biosynthesis, and functions in pollination," Protoplasma, 228, 31-39 (2006).

Pacini, E. and Hesse, M. "Pollenkitt – its composition, forms and functions," Flora (200), 399-415 (2005).

Vinzenz, X., Hüger, E., Himmerlich, M., Krischok, S., Busch, S., Wöllenstein, J. and Hoffmann C. "Preparation and characterization of poly(L-histidine)/poly(L-glutamic acid) multilayer on silicon with nanometer-sized surface structures," Journal of Colloid and Interface Science, 386, 252-259 (2012)

Wasisto, H.S., Merzsch, S., Waag, A., Uhde, E., Salthammer, T., Peiner, E., "Airborne engineered nanoparticle mass sensor based on a silicon resonant cantilever," Sensors and Actuators B: Chemical in press (2012), http://dx.doi.org/10.1016/j.snb.2012.04.003.

Zinkl, G. M., Zwiebel, B. I., Grier, D. G. and Preuss, D. "Pollen-stigma adhesion in Arabidopsis: a species-specific interaction mediated by lipophilic molecules in the pollen exine," Development, 126, 5431-5440 (1999).